Dynamics of Reaction of [5,10,15,20-Tetrakis(2,6-dimethyl-3-sulfonatophenyl)-porphinato]iron(III) Hydrate with *t*-BuOOH in Aqueous Solution. 3. Comparison of Refined Kinetic Parameters and D_2O Solvent Isotope Effects to Those for [5,10,15,20-Tetrakis(2,6-dichloro-3-sulfonatophenyl)-porphinato]iron(III) Hydrate and Iron(III) Hydrate

Enona Gopinath and Thomas C. Bruice*

Contribution from the Department of Chemistry, University of California at Santa Barbara, Santa Barbara, California 93106. *Received September 7, 1990*

Abstract: The decomposition of *t*-BuOOH in the presence of added ferric ion has been studied in buffered H_2O and D_2O solutions between pH(D) 1 to 4, by using 2,2'-azinobis(3-ethylbenzthiazolinesulfonate) (ABTS) to trap the oxidizing products. The reaction is first-order in both [*t*-BuOOH] and $[Fe^{III}]_{total}$. The value of the second-order rate constants in H_2O (k_2^H = 29 M^{-1} s^{-1}) and in D_2O (k_2^D = 15 M^{-1} s^{-1}) is independent of $H^+(D^+)$ and added buffer species but exhibits a solvent deuterium kinetic isotope effect (k_2^H/k_2^D) of 1.9. At pH(D) < 3, the second-order rate constants for reaction of [5,10,15,20-tetrakis-(2,6-dimethyl-3-sulfonatophenyl)porphinato]iron(III) [(**1**)$Fe^{III}(H_2O)_2$] with *t*-BuOOH and the reaction of [5,10,15,20-tetrakis(2,6-dichloro-3-sulfonatophenyl)porphinato]iron(III) [(**2**)$Fe^{III}(H_2O)_2$] with H_2O_2 exhibit the very same independence upon $H^+(D^+)$ and kinetic isotope effects (k_{ly}^H/k_{ly}^D) of 2.7 and 3.0, respectively. Thus, below pH 3 the reactions of Fe^{III}, (**1**)$Fe^{III}(H_2O)_2$, and (**2**)$Fe^{III}(H_2O)_2$ with *t*-BuOOH all display sizable deuterium solvent isotope effects and an independence of rate on $[H^+]$ suggesting a common mechanism. We suggest a homolytic mechanism with either $H^\bullet$ or H^+ transfer rate controlling. In the low pH region, the calculated second-order rate constant for the reaction of ferric ion with *t*-BuOOH exceeds that for the reaction of (**1**)$Fe^{III}(H_2O)_2$ with *t*-BuOOH by 5-fold. Above pH 3, a plot of the second-order rate constant (k_{ly}) vs pH, for reaction of *t*-BuOOH with H_2O and HO^- ligated $[(\mathbf{1})Fe^{III}]^+$, shows that k_{ly} increases and then decreases with increase in pH to form a bell-shaped plot with maximum k_{ly} at pH 7.0. In the mid pH range the decomposition of the critical intermediates to products is not associated with a deuterium solvent isotope effect. With further increase in pH, log k_{ly} again increases to reach a second maxima. The very same log k_{ly} vs pH profile has been seen for the reaction of *t*-BuOOH with H_2O and HO^- ligated $[(\mathbf{2})Fe^{III}]^+$. On the basis of the percentage yields of $(CH_3)_2C{=}O$ and CH_3OH the reactions above pH 3 must reflect rate-determining *t*-BuO–OH bond homolysis. Reaction mechanisms are discussed in terms of the structures of steady-state intermediates and the ground-state structures of oxidized iron porphyrin species as determined in the previous paper in this issue by Kaaret, Zhang, and Bruice. The pH-dependent second-order rate constants (k_{ly}) for the decomposition of *t*-BuOOH by $[(\mathbf{2})Fe^{III}(X)_2$, X = OH^- or $H_2O]$ exceed k_{ly} values for the reaction of $[(\mathbf{1})Fe^{III}(X)_2$, X = OH^- or $H_2O]$ with *t*-BuOOH by at most 2.5–3.8-fold across the entire pH range. The marked influence of ionic strength on the pK_a associated with (**1**)$Fe^{III}(H_2O)_2 \rightleftharpoons$ (**1**)$Fe^{III}(H_2O)(HO) + H^+$ has been determined, and from the Debye–Huckel equation for a monobasic acid the thermodynamic pK_a = 7.3 and the charge on the $Fe^{III}(H_2O)(HO)$ moiety is 2–.

Introduction

This study is part of an ongoing investigation[1] into the reactions of water-soluble, non-μ-oxo dimer-forming tetraphenyliron(III) porphyrins with alkyl and acyl hydroperoxides in aqueous solution. Previous investigations have shown that the second-order rate constants (k_{ly}) for the reactions of [5,10,15,20-tetrakis(2,6-dimethyl-3-sulfonatophenyl)porphinato]iron(III) hydrate [(**1**)-$Fe^{III}(X)_2$ (X = H_2O or OH^-)] with acyl or alkyl hydroperoxides, YOOH, exhibit different dependence upon the acidity of the YOH leaving group.[1,2] Thus, a plot of log k_{ly} vs the pK_a of YOH exhibits a definitive break at pK_a of about 11. Since heterolytic O–O bond breaking is acknowledged for the reactions of acyl hydroperoxides,[2-4] a possible explanation for the break in the linear-free energy plot would involve homolytic O–O bond cleavage with alkyl hydroperoxides. This suggestion has been challenged by allegations that (i) pK_a values of YOH species, critical to the linear-free energy plot, have been incorrectly calculated[5] and (ii) alkene epoxidation in the presence of hydroperoxides and iron(III) porphyrins results from the reaction of iron(IV)–oxo porphyrin π-cation radical and alkene[6]—the latter being formed via heterolytic O–O bond cleavage of the hydroperoxide on reaction with the iron(III) porphyrin species. Since the mechanisms of these reactions are presently of wide concern, the criteria for the assertions (i) and (ii) must be considered. The contents of the footnote[7] allow the interested reader to carry out a "back of the envelope" calculation of the questioned pK_a values for $Ph_2C(CO_2Me)OH$ and $Ph_2C(CN)OH$ such that assertion (i) will be seen to be fallacious. Concerning (ii), Labeque and Marnett[8] have demonstrated that, in the reaction of *meso*-tetraphenylporphinatoiron(III) with a fatty acid alkyl hydroperoxide, only products resulting from homolytic cleavage of the hydroperoxide O–O bond are formed and also that the epoxidation of *cis*-stilbene produces mostly *trans*-stilbene oxide, which implicates the hydroperoxyl radical in the epoxidation reaction. It was proposed that the hydroperoxyl radical is formed in these systems due to the oxidation of hydroperoxide by the primary products of the

(1) Bruice, T. C. In *Mechanistic Principles of Enzyme Activity*; Lieman, J. F., Greenburg, A., Eds.; VCH Publishers: New York, 1988; p 227.
(2) Balasubramaninan, P. N.; Lee, R. W.; Bruice, T. C. *J. Am. Chem. Soc.* **1989**, *111*, 8714.
(3) Lindsey-Smith, J. R.; Balasubramanian, P. N.; Bruice, T. C. *J. Am. Chem. Soc.* **1988**, *110*, 7411.
(4) Balasubramanian, P. N.; Lindsey-Smith, J. R.; Davies, M. J.; Kaaret, T. W.; Bruice, T. C. *J. Am. Chem. Soc.* **1989**, *111*, 1477.
(5) Traylor, T. G.; Ciccone, J. P. *J. Am. Chem. Soc.* **1989**, *111*, 8413.
(6) Traylor, T. G.; Fann, W.-P.; Bandopadhyay, D. *J. Am. Chem. Soc.* **1989**, *111*, 8009.
(7) pK_a of MeOH = 15.5 (Ballinger and Long, *J. Am. Chem. Soc.* **1960**, *82*, 795), ρ^I = −8.4 (Fox and Jencks, *J. Am. Chem. Soc.* **1974**, *96*, 1436), σ_I for Ph– = 0.2, for CN– = 0.56, and for CO_2Me– = 0.34 (Charton, M. *J. Org. Chem.* **1964**, *29*, 1222).
(8) Labeque, R.; Marnett, L. J. *J. Am. Chem. Soc.* **1989**, *111*, 6621.

0002-7863/91/1513-4657$02.50/0

Scheme I[a]

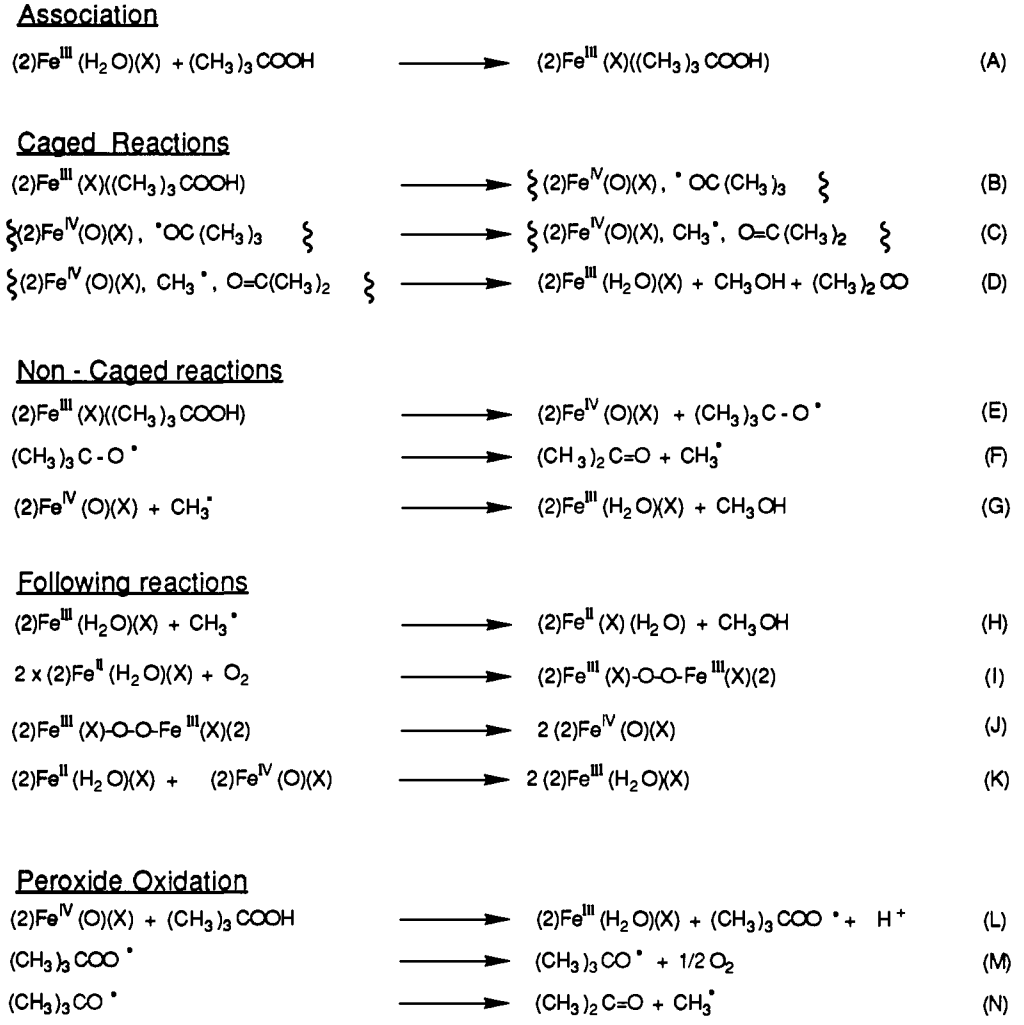

[a] Where X = H_2O or OH^-.

reaction of metalloporphyrin and hydroperoxide (RO• and (porph)Fe^{IV}=O). Additional observations on this topic will be forthcoming from our laboratory.[9]

The results of prior investigation[3,4,18] of the kinetics and products of the reaction of alkyl hydroperoxides with (**1**)$Fe^{III}(X)_2$ and tetrakis(2,6-dichloro-3-sulfonatophenyl)porphinatoiron(III) hydrate [(**2**)$Fe^{III}(H_2O)(X)$, X = H_2O, HO^-] have led to the proposal that the reactions of Scheme I predominate at neutral pH. In Scheme I the products of the "caged reactions" and "noncaged reactions" are identical, but the two sets of reactions may be differentiated by the ability (product yields and the kinetics for trapping) of the easily $1e^-$ oxidizable reagent 2,2′-azinobis(3-ethylbenzthiazolinesulfonate) (ABTS) to reduce *t*-BuO• → *t*-BuOH and (porph)$Fe^{IV}(O)(X)$ → (porph)$Fe^{III}(H_2O)$ generated only in the noncaged reaction. The validity of the caged reaction would require the fragmentation of *t*-BuO• to take place, associated with (porph)$Fe^{IV}(O)(X)$ in the cage, with a rate constant of ca. 1.7×10^8 s^{-1} as compared to a rate constant of 1.4×10^6 s^{-1} when *t*-BuO• is free in water.[10,11] The (porph)$Fe^{II}(H_2O)(X)$ proposed in the "following reactions" has been shown to be formed by trapping with CO to give (porph)$Fe^{II}(CO)(X)$. The formation of observable concentrations of (porph)$Fe^{IV}(O)(X)$ has been shown to require the presence of O_2. [In the heterolytic O–O bond cleavage which accompanies the reaction of acyl hydroperoxides with (porph)$Fe^{III}(X)_2$, O_2 is not required for the formation of (porph)$Fe^{IV}(O)(X)$.] In relation to the "peroxide oxidation" reactions of Scheme I (i) the kinetics of the oxidation of hydroperoxides by (porph)$Fe^{IV}(O)(X)$ have been studied and (ii) the formation of CH_4, C_2H_6, O_2, or (*t*-BuO)$_2$ is not observed. The latter observation is in accord with reactions (M) and (N) which are apparently favored in H_2O, in preference to 2*t*-BuOO• → (*t*-BuO)$_2$ + O_2.

In order to gain a thorough understanding of the reactions of iron(III) porphyrins with oxygen donors in water it is desirable to have a detailed knowledge of the dependency of the apparent second-order rate constant on acidity, transfer from H_2O to D_2O and the presence of general acid and base species. We have now investigated the acidity dependence of the rates of reaction[12,13] of *t*-BuOOH with (**1**)$Fe^{III}(X)_2$ and with iron(III) in H_2O and D_2O and compared the pH dependence of rate constants for the reactions of iron(III), (**1**)$Fe^{III}(X)_2$ and (**2**)$Fe^{III}(X)_2$. Reactions have been considered in terms of the finding that in water the axial ligands to porphyrin iron(III) and iron(IV) species are H_2O and HO^- rather than the oxo species (Fe=O). The influence of ionic strength and transfer from H_2O to D_2O on the acid dissociation

(9) He, G. X.; Bruice, T. C., unpublished results.

(10) Erben-Russ, M.; Michael, C.; Bors, W.; Saran, M. *J. Phys. Chem.* **1987**, *91*, 2362.

(11) CH_3• formed from the fragmentation of *t*-BuO•, has been shown to be oxidized → CH_3OH by Fe^{III} porphyrin as well as by an Fe^{IV} porphyrin: Brault, D.; Neta, P. *J. Am. Chem. Soc.* **1981**, *103*, 2705.

(12) In a previous report[3] of the pH dependence of the second-order rate constant for reaction of *t*-BuOOH with (**1**)$Fe^{III}(X)_2$ (X = H_2O or HO^-), errors were introduced by the presence of ammonium ion as the counter ion to the anionic ABTS trapping agent and about 1% ferric ion impurity in the (**1**)-$Fe^{III}(X)_2$ sample employed. Ammonia and certain primary amines are now known to potentiate the reaction of (**1**)$Fe^{III}(X)_2$ with *t*-BuOOH.[11] These errors have been corrected in the present study by use of the sodium salt of ABTS as a trap for oxidizing intermediates and the purification of (**1**)$Fe^{III}(X)_2$ by ultrafiltration.

(13) Beck, M. J.; Gopinath, E.; Bruice, T. C., unpublished results.

constant for (1)$Fe^{III}(H_2O)_2 \rightarrow$ (1)$Fe^{III}(HO)(H_2O) + H^+$ have been determined.

In the preceding paper in this issue[14] we show that in water the oxygen ligands of $[(1)Fe^{III}]^+$, $[(1)Fe^{IV}]^{2+}$, and $[(1^{\bullet})Fe^{IV}]^{3+}$ are H_2O and HO^- and that the oxo ligand may only be important at high pH where (1)$Fe^{IV}(HO)_2$ and $(1^{+\bullet})Fe^{IV}(HO)_2$ cannot be differentiated from (1)$Fe^{IV}(=O)(H_2O)$ and $(1^{+\bullet})Fe^{IV}(=O)(H_2O)$. Mechanisms are discussed with this in mind as well as the pH dependence of deuterium solvent kinetic isotope effects and the pH dependence of reactions.

Experimental Section

Materials. Deionized, double glass distilled water was used for all experiments. Buffer and salt solutions were prepared from reagent grade chemicals and either passed over a chelex column (buffers of pH > 7) or extracted with 0.01% dithiazone in dichloromethane to remove any heavy metal contamination. 2,2′-Azinobis(3-ethylbenzthiazoline-6-sulfonic acid), disodium salt (ABTS, disodium salt) was prepared from the commercially available diammoniun ABTS (Sigma) by adjusting a dilute solution of the diammoniun salt to 1 M in Na^+ by addition of 2 M $NaNO_3$. The precipitate of the disodium salt was then collected, redissolved in H_2O, and twice reprecipitated in the same manner. The disodium ABTS so obtained was immediately dried in vacuo over P_2O_5. $Fe^{III}Cl_3 \cdot 6H_2O$ was purchased from AEsar and used as received. Concentrations of stock solutions of $Fe^{III}Cl_3$ were determined by quantitating the UV absorbance of 1,10-phenanthroline complexes.[15] Deuterium oxide (99.9%) was from Aldrich. Deuterated buffers were prepared by rotory evaporation of aqueous buffer solutions, dissolving the residual salt in D_2O and evaporating to dryness. The latter procedure was repeated three times prior to reconstituting the buffer in D_2O. Preparation and purification of (1)$Fe^{III}(X)_2$ used was described in the preceding paper in this issue.[14]

Instrumentation. Kinetic studies were conducted by using either Perkin-Elmer 553 or Uvikon 810 UV-vis spectrophotometers with cell compartments thermostated at 30 °C. Anaerobic experiments were performed in a glovebox under a nitrogen atmosphere. Spectrophotometric titrations were conducted in a titration cell fitted with a Corning pencil-thin, polymer body electrode, in the thermostated cell compartment of a Perkin-Elmer 553 spectrophotometer. pH measurements were performed with a Radiometer Model 26 pH meter.

Results

The influence of change from H_2O to D_2O on the pK_a of (1)-$Fe^{III}(Y_2O)_2$ (Y = H or D) was determined under the same conditions of temperature and ionic strength (30 °C, and μ = 0.2) employed in the kinetic studies. The visible absorption spectra of (1)$Fe^{III}(Y_2O)_2$ and (1)$Fe^{III}(Y_2O)(YO^-)$ species were found to be identical in H_2O and in D_2O at pH 3 and 10. Spectrophotometric titrations were carried out between pH(D) 4 and 10. Values of pD were determined by the addition of 0.38[16] to the pH meter reading. The pK_a values for the deprotonation of (1)$Fe^{III}(Y_2O)_2$ (eq 1) were obtained by fitting the change in absorbance at λ =

$$Fe^{III}(Y_2O)_2 \overset{K_{a1}}{\rightleftharpoons} Fe^{III}(Y_2O)(YO^-) + Y^+ \qquad (1)$$

393 and 414 nm, with change in pH(D) to a theoretical curve for the dissociation of a monoprotic acid, by using a least-squares-fitting routine. The pK_as are found to be 6.75 for deprotonation of (1)$Fe^{III}(H_2O)_2$ in H_2O and 7.25 for deprotonation of (1)-$Fe^{III}(D_2O)_2$ in D_2O (Figure 1).

The influence of ionic strength on the pK_a values of (1)Fe^{III}(-$H_2O)_2$ in water was determined over a 10^4 range of ionic strengths. The objectives being to determine both the dependence of the pK_a on ionic strength and the value of the thermodynamic pK_a at zero ionic strength. Spectrophotometric titrations were carried out, and the data were analyzed in the manner described (loc. cit.). For the dissociation of any acid $HA^{(n-1)-}$ to provide $a^{n-} + H^+$, the relationship of the observed pK_a' at any ionic strength μ to the thermodynamic pK_a is described by eq 2, which is obtained by using Güntelberg's form of the Debye–Huckel equation for the single-ion activities.[17] A plot of pK_a' vs $0.5\mu^{1/2}/(1 + \mu^{1/2})$, where p$K_a'$ is the determined pK_a at ionic strength μ, is linear (Figure 2) to μ = 1.0. The y-axis intercept provides the pK_a (7.3), and

(14) Kaaret, T. W.; Zhang, G.-H.; Bruice, T. C. *J. Am. Chem. Soc.*, preceding paper in this issue.

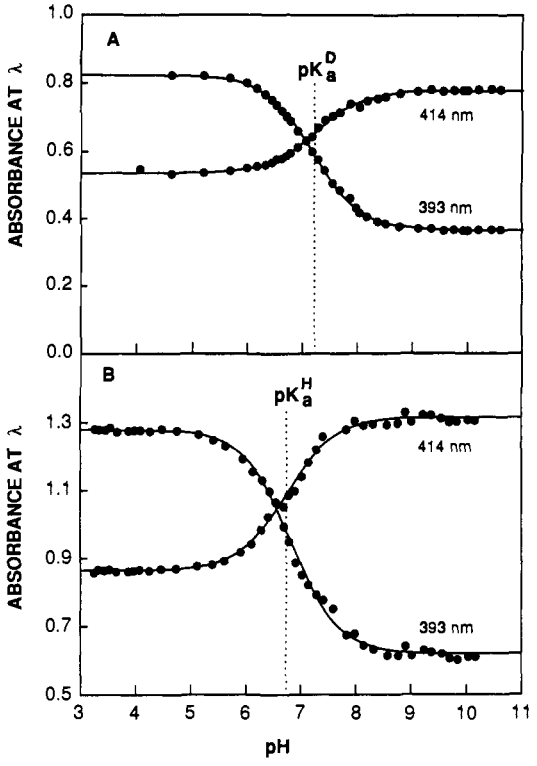

Figure 1. Absorbance vs pH plots from spectrophotometric titrations of (a) (1)$Fe^{III}(H_2O)_2$ (1×10^{-5} M) in H_2O (bottom) and (b) (1)$Fe^{III}(D_2O)_2$ (6×10^{-6} M) in D_2O (top), at 30 °C and ionic strength = 0.2 (kept constant with $NaNO_3$). The points are experimental, and the lines are computer-generated by using the appropriate equation for absorbance change with pH, for the dissociation of a monoprotic acid.

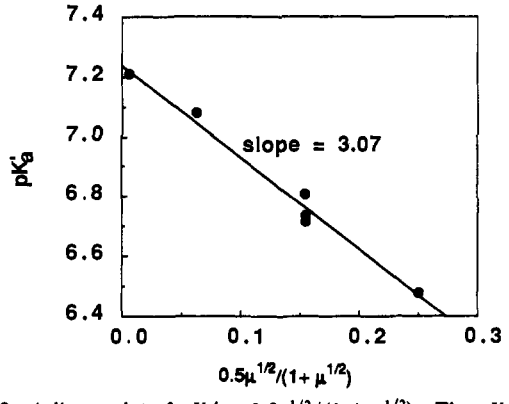

Figure 2. A linear plot of pK_a' vs $0.5\mu^{1/2}/(1 + \mu^{1/2})$. The p$K_a'$ is the determined pK_a at 30 °C and ionic strength μ, determined by spectrophotometric titration of (1)$Fe^{III}(H_2O)_2$ ⇌ (1)$Fe^{III}(H_2O)(OH) + H^+$. Concentrations of (1)$Fe^{III}(H_2O)(X)$ ranged from 4–6 × 10^{-6}, and ionic strength was maintained with $NaNO_3$.

the slope of this linear plot is equal to $-(2n - 1) = -3$ such that $n = 2$.

$$pK_a' = pK_a - (2n-1)0.5\mu^{1/2}/(1 + \mu^{1/2}) \qquad (2)$$

The kinetics of the reaction of *tert*-butyl hydroperoxide with (1)$Fe^{III}(X)_2$ (30 °C, μ = 0.2) were determined spectrophotometrically, as previously described,[3] by following the increase in absorbance of $ABTS^{\bullet+}$ (660 nm). A typical reaction mixture contained (1)$Fe^{III}(X)_2$ in concentrations ranging from 5×10^{-7} to 1.2×10^{-5} M, in a buffered solution containing 6×10^{-3} M ABTS. Buffers employed were $ClCH_2COO^-/ClCH_2COOH$ (pH 1.7–3.7), CH_3COO^-/CH_3COOH (pH 3.7–5.2), $H_2PO_4^-/HPO_4^{2-}$ (pH 5.7–7.8), HCO_3^-/CO_3^{2-} (pH 8.9–10.5), and H_2O/HO^- (above pH 10.5). Reactions were initiated by addition of *t*-BuOOH to a final concentration of 6×10^{-5} M. The appearance of $ABTS^{\bullet+}$ followed the first-order rate law to completion of

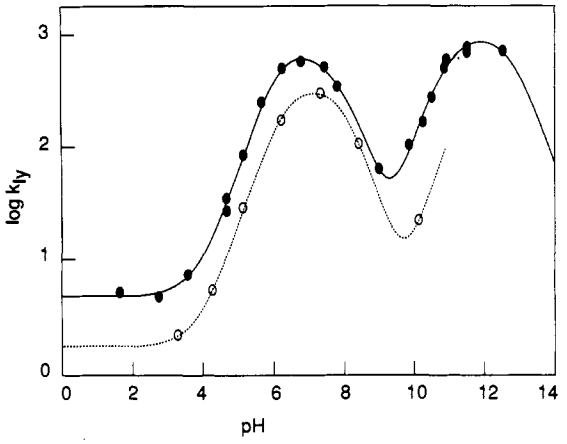

Figure 3. Plots of k_{ly}^{H} (—●—) and k_{ly}^{D} (- -○- -), for the reactions of *t*-BuOOH(D) with (**1**)$Fe^{III}(X)_2$ vs pH(D). The lines are computer-generated by iterative fitting of the points to eq 3. The values of constants that provided the optimal fits shown are presented in Table I.

reactions between pH 4.0 and 8.0. At pH values <4 and >8 the kinetics were somewhat more complex. At low pH values, ABTS is oxidized to $ABTS^{\bullet+}$ in the presence of O_2. This problem was minimized by running the reactions in a glovebox under nitrogen atmosphere. On occasion, traces of O_2 remaining in solution brought about a small zero-order drift, which was corrected for by use of a program for simultaneous zero- and first-order reactions to fit the plot of A_{660} vs time. At high pH values, $ABTS^{\bullet+}$ is increasingly susceptible to oxidation to the colorless $ABTS^{2+}$. In these cases the first-order rate constants for ABTS → $ABTS^{\bullet+}$ → $ABTS^{2+}$ were obtained by the fitting of A_{660} vs time plots to the appropriate rate expression for two sequential first-order reactions. Such fitting of kinetic data was carried out, at each pH investigated, by using five to six values of [(**1**)$Fe^{III}(X)_2$] which spanned a 10-fold concentration range. At all pH values, the rate constants (k_{obsd}) for ABTS → $ABTS^{\bullet+}$ were linearly dependent on (**1**)$Fe^{III}(X)_2$. Second-order rate constants (k_{ly}^{H}) were obtained from the slopes of the linear plots of k_{obsd} vs [(**1**)$Fe^{III}(X)_2$]. At pH's below 3 and above 10, plots of k_{obsd} vs [(**1**)$Fe^{III}(X)_2$] were found to have nonzero intercepts. This indicates that there is a slow decomposition of *t*-BuOOH which is independent of the presence of iron(III) porphyrin. This may be attributed to residual traces of metal ions remaining in the demetalated buffer solutions. No buffer catalysis was detected with $ClCH_2COO^-$/$ClCH_2COOH$, CH_3COO^-/CH_3COOH, $H_2PO_4^-$/HPO_4^{2-}, and HCO_3^-/CO_3^{2-} buffers. Twenty-one values of k_{ly}^{H} were determined at pH values ranging from 1.7 to 12.8.

Kinetic runs and the determination of first- and second-order rate constants in D_2O (k_{obsd}^{D} and k_{ly}^{D}) were carried out under the same conditions as described for H_2O. Preparation of deuterated buffers is described in the Experimental Section. Rate constants were determined at seven different pD values ranging from 3.3 to 10.3. It was not possible to obtain k_{ly}^{D} above pD 10.3 by this method, due to a solvent kinetic isotope effect such that the rates of oxidation of $ABTS^{\bullet+}$ → $ABTS^{2+}$ approach the k_{obsd}^{D} values for ABTS → $ABTS^{\bullet+}$ so that very little change in A_{660} is seen. In Figure 3 the values obtained for k_{ly} in H_2O and in D_2O (i.e., k_{ly}^{H} and k_{ly}^{D}) are plotted as a function of pH(D).

Kinetic Studies of the reaction of $Fe^{III}Cl_3$ with *tert*-butyl hydroperoxide in H_2O and in D_2O at low pH were performed under the same conditions of temperature, ionic strength, and *t*-BuOOH and ABTS concentrations as well as the same range of catalyst concentrations as described for (**1**)$Fe^{III}(X)_2$. Due to the usual problem of the precipitation of hydrated iron(III) species, reactions were investigated between pH(D) 1.0 and 3.7. Reactions followed the first-order rate law in the formation of $ABTS^{\bullet+}$ to at least 90% completion of reaction (Figure 4). Values of the first-order rate constants (k_{obsd}) obtained over a 10-fold range of Fe^{III} concentrations are linearly dependent on the concentration of added $FeCl_3$ at the pH(D) values examined (Figure 5). Second-order rate constants (k_2) were calculated from the slopes of the plots

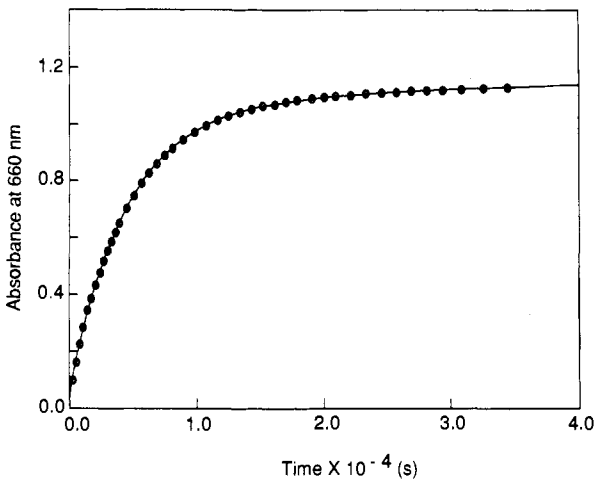

Figure 4. A plot of the change in absorbance at 660 nm vs time for the reaction of Fe^{III} (5.34×10^{-6} M) with *t*-BuOOH at pH 2.7. The points are experimental, and the line fitting the points is generated from the first-order rate equation.

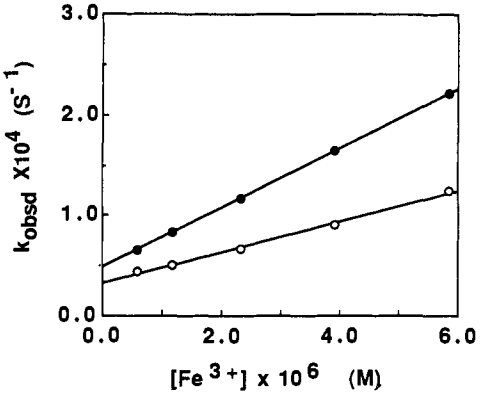

Figure 5. Plots of observed first-order rate constants vs [Fe^{III}] for the Fe^{III}-catalyzed oxidation of ABTS by (a) *t*-BuOOH in H_2O at pH 1.7 (●) and (b) *t*-BuOOD in D_2O at pD 3.3 (○). The initial concentrations of *t*-BuOOH and ABTS were 6×10^{-5} and 6×10^{-3} M, respectively.

of k_{obsd} vs added $FeCl_3$. Values of k_2 were found to be pH(D) independent between pH(D) 1.0 and 3.0. The value of the deuterium solvent kinetic isotope effect $k_2^{H}/k_2^{D} = 29/15 \approx 1.9$.

Discussion

The objective of the present investigation has been to gather information that would lead to a better understanding of the mechanism for the reaction of *t*-BuOOH with iron(III) and iron(III) tetraphenylporphyrins. The iron(III) porphyrin of this study is [5,10,15,20-tetrakis(2,6-dimethyl-3-sulfonatophenyl)-porphinato]iron(III) hydrate [(**1**)$Fe^{III}(X)_2$ (X = Y_2O or YO^-, Y = H or D)]. The kinetic studies were in H_2O and D_2O at 30 °C and μ = 0.2 ($NaNO_3$).

The effect of ionic strength on the pK_{a1} for the acid dissociation of (1)$Fe^{III}(H_2O)_2$ to (1)$Fe^{III}(OH)(H_2O)$: Since the apparent second-order rate constants for reaction of (**1**)$Fe^{III}(X)_2$ with *t*-BuOOH ($k_{ly}^{H(D)}$) are dependent upon the mole fraction of the iron(III) porphyrin as (**1**)$Fe^{III}(Y_2O)_2$ and (**1**)$Fe^{III}(YO^-)(Y_2O)$ species (Y = H or D), we have determined the influence of ionic strength on the pK_a of (**1**)$Fe^{III}(H_2O)_2$ in H_2O (eq 2). From the relationship of μ to pK_a' (Debye–Huckel equation) the acid dissociation of (**1**)$Fe^{III}(H_2O)_2$ ⇌ (**1**)$Fe^{III}(H_2O)(OH)$ + H^+ was found to be that expected for the ionization of an acid HA^{1-} ⇌ A^{2-} + H^+. The metal center of (**1**)$Fe^{III}(H_2O)(OH^-)$ is ligated to a porphyrin dianion and to a hydroxide anion, and therefore there should be a net zero charge on the metal. Each of the four phenyl groups, at the meso positions of the tetraphenylporphyrin, carry a negatively charged *m*-SO_3^- substituent. Further work will be directed toward determining if charged meta substituents exert a partial negative or positive charge on the metal center. If this

Table I. Values of Rate and Equilibrium Constants Obtained from the Fitting of Eq 3 to the Experimental Points in Figure 1

kinetic terms	values of determined constants in reaction of (1)$Fe^{III}(X)_2$ with *t*-BuOOH in H_2O	*t*-BuOOD in D_2O set 1	*t*-BuOOD in D_2O set 2	D_2O solvent isotope effects (H/D) set 1	D_2O solvent isotope effects (H/D) set 2
$k_1k_2/(k_2 + k_{-1})$	5.0	1.8	1.8	2.8	2.7
$(k_4/k_2)K_{a3}$	1.4×10^{-4}	1.2×10^{-4}	1.1×10^{-4}	1.1	1.2
k_3/k_1	0.44	1.0	0.13	0.4	3.2
$(k_4 + k_{-3})K_{a3}/(k_2 + k_{-1})$	5.5×10^{-7}	5.2×10^{-7}	3.0×10^{-7}	1.0	1.7
$(k_6 + k_{-5})K_{a4}/(k_4 + k_{-3})$	1.1×10^{-8}	1.1×10^{-8}	6.5×10^{-10}	1.0	17
K_{a1}	1.8×10^{-7}	5.6×10^{-8}	5.6×10^{-8}	3.2	3.2
$k_6k_5K_D/(k_6 + k_{-5})$	71.1				
K_{a2}	1.2×10^{-11}				
K_b	1.6×10^{-13}				

Scheme II[a]

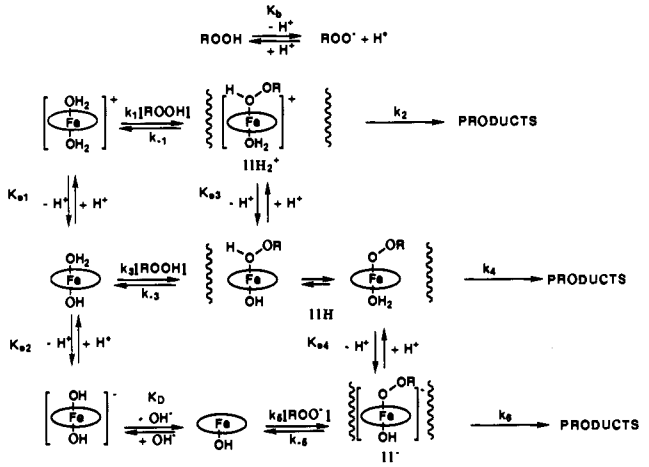

[a] All Fe are in the 3+ oxidation state.

is found to be the case it would indicate that charged groups at some distance from the catalytic center influence the electrostatic charge of the center and could control aspects of mechanisms for reaction at the metal center.

The pH dependences of the second-order rate constants for the reaction of *t*-BuOOH with (1)$Fe^{III}(X)_2$ in H_2O and D_2O (k_{ly}^H and k_{ly}^D) are shown in Figure 3. The data points in Figure 3 are experimental, and the lines are generated from eq 3 by using the values of constants reported in Table I. Equation 3 is derivable

$$k_{ly} = A + B + C \tag{3}$$

$$A = \frac{k_2k_1}{(k_2 + k_{-1})}$$

$$B = \frac{\dfrac{k_2k_1}{(k_2 + k_{-1})}\left\{\dfrac{k_4K_{a3}a_H^2}{k_2} + \dfrac{k_4k_3K_{a3}K_{a1}a_H}{k_2k_1}\right\}}{\left\{a_H^2 + \dfrac{(k_4 + k_{-3})a_HK_{a3}}{(k_2 + k_{-1})} + \dfrac{(k_6 + k_{-5})K_{a3}K_{a4}}{(k_2 + k_{-1})}\right\}(a_H + K_{a1})}$$

$$C = \frac{\left\{\dfrac{k_6k_5K_DK_{a2}K_b}{(k_6 + k_{-5})K_w}\right\}a_H}{(a_H + K_{a2})(K_b + a_H)}$$

from the reaction sequences of Scheme II, where the reaction proceeds through paths I, II, III, and IV shown in Scheme III where intermediates IIH_2^+, IIH, and II^- are at low steady-state concentrations. The derivation of eq 3 has been discussed in a previous manuscript dealing with the reaction of *t*-BuOOH with 5,10,15,20-tetrakis(2,6-dichloro-3-sulfonatophenyl)iron(III) hydrate [(2)$Fe^{III}(X)_2$].[18]

Scheme III

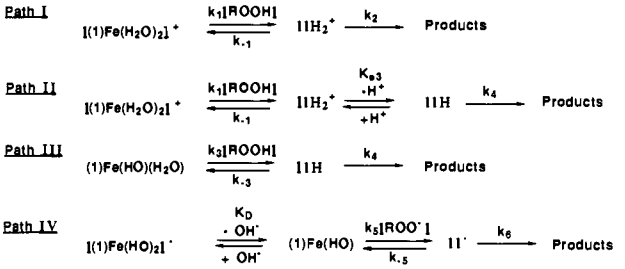

The pK_{a1} for the $H^+(D^+)$ ionization of (1)$Fe^{III}(X)_2$ (pK_{a1}) was experimentally determined and the pK_a of *tert*-butyl hydroperoxide (pK_b) has been reported in the literature.[19] All other rate and equilibrium constant terms in Table I were obtained by iterative fitting of the experimental data to eq 3.

In the pH vs log rate constant profiles of Figure 3, the filled circles are values of k_{ly}^H, and the solid line which fits the points has been generated by using the constants in column 2 of Table I, while the empty circles represent values of k_{ly}^D and the dashed line which fits these points was generated from eq 3 by use of the constants presented in column 3 (either set 1 or set 2) of Table I.

Inspection of Figure 3 shows the pH profile of k_{ly}^H to be resolved into three distinct portions: (i) a plateau at low pH (<3) where k_{ly} is independent of acidity, (ii) a "bell-shaped" region in the intermediate region (pH 3–9), and (iii) a second bell-shaped region at high pH (pH 9–13). Equation 3, which describes the profile is seen to be a sum of three terms, each representing one of the regions. In the plateau region (pH < 3), k_{ly}^H is described by eq 4, which simplifies to the first term (*A*) of eq 3 at low pH, and

$$k_{ly} = \frac{k_1k_2a_H}{(k_{-1} + k_2)(a_H + K_{a1})} = \frac{Aa_H}{(a_H + K_{a1})} \tag{4}$$

the reaction proceeds through path I of Scheme III. The bell-shaped region at intermediate pH is described by the middle term (*B*) in eq 3, which itself is the sum of two terms. A general form of an equation that provides a bell-shaped dependence of a rate constant on pH is described by eq 5a. Inspection of eq 5a shows the ascending leg to be due to an acid dissociation associated with

$$k_{ly} = \frac{k_rK_{ad}a_H}{(a_H + K_{aa})(a_H + K_{ad})} \tag{5a}$$

pK_{aa} and the descending leg to be due to an acid dissociation associated with pK_{ad}. Each of the two parts of term B of eq 3 which describe the "bell" at intermediate pH can be seen to reduce to the mathematical form of eq 5a at appropriate pH values. Thus, at pH values < pK_{a4} the first term simplifies to eq 5b and the

(15) Harvey, A. E.; Smart, J. A.; Amis, E. S. *Anal. Chem.* **1955**, *27*, 26.
(16) Fife, T. H.; Bruice, T. C. *J. Phys. Chem.* **1961**, *65*, 1079.
(17) (a) Stumm, W.; Morgan, J. J. *Aquatic Chemistry*; Halsted Press; John Wiley and Sons, Inc.: New York, 1981; p 136. (b) Robinson, R. A.; Stokes, R. H. *Electrolyte Solutions*; Butterworths Publications, Ltd.: 1959; p 231.
(18) Murata, K.; Panicucci, R.; Gopinath, E.; Bruice, T. C. *J. Am. Chem. Soc.* **1990**, *112*, 6072.
(19) Everett, A. J.; Minkoff, G. J. *Trans. Faraday Soc.* **1953**, *49*, 410.

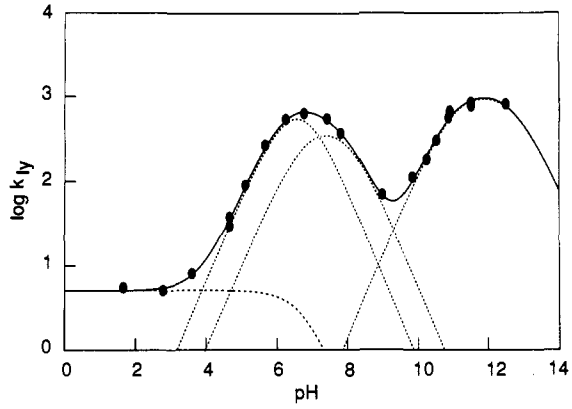

Figure 6. The solid circles denote k_{ly}^{H} values for the reactions of *t*-BuOOH with (1)$Fe^{III}(X)_2$ (—●—) vs pH. The solid line is generated from eq 3, by using the constants reported in Table I. The dotted lines represent the contributions of the individual terms of eq 3 (from left to right): term A (plateau term at low pH), eq 5b (first bell), eq 5c (second bell), and term C (third bell).

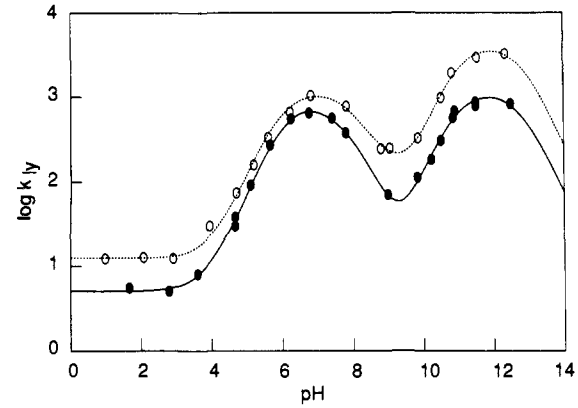

Figure 7. A plot of k_{ly}^{H} values for the reactions of *t*-BuOOH with (1)$Fe^{III}(X)_2$ (—●—, this study) and with (2)$Fe^{III}(X)_2$ (--○--, ref 18) vs pH. The two sets of points are experimental, and the lines are obtained by computer fitting of the experimental points by using eq 3. The set of constants used to generate the solid line are provided in Table I, and those that produce the dashed line are from ref 18.

reaction proceeds mostly through path II of Scheme III, and at pH > pK_{a3} the second term simplifies to eq 5c, which represents

$$k_{ly} = \frac{\frac{k_4 k_1 K_{a3} a_H}{(k_2 + k_{-1})}}{\left\{a_H + \frac{(k_4 + k_{-3})}{(k_2 + k_{-1})} K_{a3}\right\}(a_H + K_{a1})} \quad (5b)$$

$$k_{ly} = \frac{\frac{k_4 k_3 K_{a1}}{(k_4 + k_{-3})} a_H}{\left\{a_H + \frac{(k_6 + k_{-5})}{(k_4 + k_{-3})} K_{a4}\right\}(a_H + K_{a1})} \quad (5c)$$

the reaction of path III of Scheme III. We may conclude that the bell at intermediate pH is, in reality, two overlapping bells, such that the kinetically apparent acid dissociation constant (k_{app1}) associated with the ascending leg of the bell (pH 3–5) is actually equal to $K_{a3}(k_4 + k_{-3})/(k_2 + k_{-1})$, while the K_{app2} associated with the descending leg (pH 7–9) is equal to $K_{a4}(k_6 + k_{-5})/(k_4 + k_{-3})$.

The second bell at high pH is described by the last term in eq 3, so that the reaction pathway is path IV. Here the ascending leg of the bell is associated with the acid dissociation of (1)-$Fe^{III}(OH)(H_2O) \rightleftharpoons$ (1)$Fe^{III}(OH)_2 + H^+$ (pK_{a2}) and its descending leg with the acid dissociation of *t*-BuOOH $\rightleftharpoons$ *t*-$BuOO^- + H^+$ (pK_b).

The terms of eqs 3 (A and C) and 5b,c additively describe the pH dependency of log k_{ly}, such that each may be plotted separately as shown by the dashed lines of Figure 6 (see legend to the figure). For the fitting of the log k_{ly} vs pH profile, the value of K_b (Table I) is that reported in the literature, whereas a K_{a2} value of 1.2×10^{-11} was obtained from the fitting of the experimental data by eq 1. That the value of K_{a2} determined by iteration is reasonable is shown by comparison to that determined electrochemically (2.8×10^{-11}) at the same ionic strength.[14]

Comparison of the Rate Constants for the Reaction of (1)-$Fe^{III}(X)_2$ and [5,10,15,20-Tetrakis(2,6-dichloro-3-sulfonatophenyl)porphinato]iron(III) Hydrate [(2)$Fe^{III}(X)_2$] with *t*-BuOOH. Figure 7 shows the pH dependence of k_{ly} values for the reactions of *t*-BuOOH with (1)$Fe^{III}(X)_2$ (filled circles, solid line) and with (2)$Fe^{III}(X)_2$ (empty circles, dashed line). The two sets of points are experimental, and the lines are generated by computer fitting of the experimental points with use of eq 3. The value for the first ionization (K_{a1}) of (1)$Fe^{III}(X)_2$ is from this study, and K_{a1} for ionization of (2)$Fe^{III}(X)_2$ is from a previous study.[18] Values for all other rate and equilibrium constant terms were obtained by iterative fitting of the data to eq 3. From Figure 7, it is seen that the rates for (2)$Fe^{III}(X)_2$ are, at most, greater than those for (1)$Fe^{III}(X)_2$ by only 2.5–3.8 fold (0.5–0.8 kcal/mol). Thus, replacing the eight ortho-methyl substituents in (1)$Fe^{III}(X)_2$ by chloro substituents (2)$Fe^{III}(X)_2$ provides only a minor difference in the reactivity toward *t*-BuOOH in H_2O.

Comparison of the Kinetic Parameters Obtained for the Reaction of *t*-BuOOH(D) with (1)$Fe^{III}(X)_2$ in H_2O and D_2O. From the pH dependences of k_{ly}^{H} and k_{ly}^{D} shown in Figure 3, values of k_{ly}^{H}/k_{ly}^{D} are seen to be 2.7 at the low pH plateau (pH 1–3), 3.1 in the ascending part of the bell (pH 5.4), 2.0 at the top of the bell (pH 7.0), and 1.5 in the descending part of the bell (pH 8.5). However, $k_{ly}^{H(D)}$ values are composed of several terms, which must be resolved to find isotope effects on individual steps of the reactions of Scheme II. The kinetic parameters required to fit eq 3 to $k_{ly}^{H(D)}$ for the reaction of *t*-BuOOH(D) with (1)$Fe^{III}(X)_2$ in H_2O and in D_2O (where X = Y_2O or YO^- and Y = H or D) are presented in Table I. For the reaction in D_2O two sets of values are provided. Both sets yield plots of log k_{ly}^{D} vs pD, which fit the experimental points closely, and illustrate the relative importance of the constants of eq 3 in determining the calculated values of k_{ly}. From a comparison of set 1 and set 2 of Table I it is seen that a deuterium kinetic isotope effect may be determined only for two terms of eq 3: $\{k_1k_2/(k_2 + k_{-1})\}$ and $\{k_4K_{a3}/k_2\}$.

The term, $(k_1^H/k_1^D)(k_2^H/k_2^D)(k_2^D + k_{-1}^D)/(k_2^H + k_{-1}^H) = 2.7–2.8$, pertains to the isotope effect of the pH-independent reaction below pH 3. The constants k_1 and k_{-1} relate to *t*-BuOOH(D) ligation to and dissociation from the iron(III) porphyrin. Therefore, k_1^H/k_1^D and k_{-1}^H/k_{-1}^D represent secondary isotope effects and should approximate unity. Also, k_2 is a commitment step such that $k_{-1} \gg k_2$ and $(k_2^D + k_{-1}^D)/(k_2^H + k_{-1}^H) \approx k_{-1}^D/k_{-1}^H \approx 1$. Therefore, the breakdown of [(1)Fe^{III}-(H_2O)(*t*-BuOOH)] (Scheme II) at low pH is associated with a solvent isotope effect $(k_2^H/k_2^D) \approx 2.7$. A deuterium solvent isotope effect of 2.7–2.8 is expected for a reaction which involves H^+/D^+ transfer to and from oxygen.

The term $\{k_4K_{a3}/k_2\}$ pertains to the ascending leg of the bell at intermediate pH. The isotope effect of 1.1–1.2 (Table I) pertains to the term $(k_4^H/k_4^D)(k_2^D/k_2^H)(K_{a3}^H/K_{a3}^D)$. We earlier deduced that $(k_2^D/k_2^H) = 0.37$. Since pK_{a1} and the kinetically apparent pK_{a3} differ by less than 2, we may assume that $(K_{a3}^H/K_{a3}^D) \approx (K_{a1}^H/K_{a1}^D) = 3.2$ such that $(k_4^H/k_4^D) \approx 1$. Thus there appears to be no kinetic isotope effect on the breakdown of [(1)$Fe^{III}(HO)$(*t*-BuOOH)/(1)$Fe^{III}(H_2O)$(*t*-BuOO)] at intermediate pH values.

Of the other terms of eq 3, the apparent pK_a for *t*-BuOOD ligated to iron(III) porphyrin $(k_4 + k_{-3})K_{a3}/(k_2 + k_{-1})$ may be determined to within a 60% range of certainty, whereas the other two kinetically determined constants $[k_3/k_1$ and $(k_4 + k_{-3})K_{a3}/(k_2 + k_{-1})]$ may be allowed to vary within an order of magnitude without significantly affecting the degree of agreement of the theoretical curve with the experimental points. The ambiguity in the determination of these constants stems from the unavail-

Scheme IV

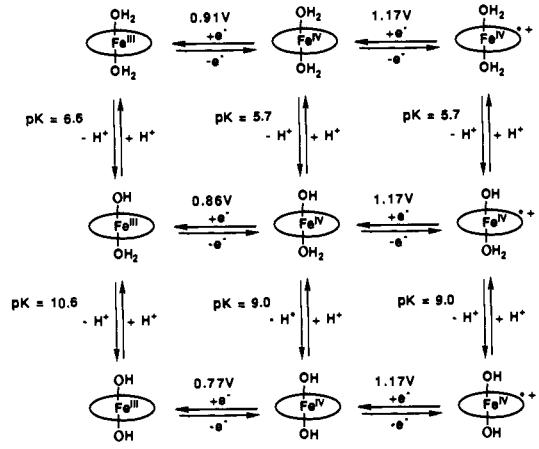

Scheme V

Reactive Complex	Thermodynamically Favored Product
(1)$Fe^{III}(H_2O)$(*t*-BuOOH)	(1)$Fe^{IV}(H_2O)_2$ or (+·1)$Fe^{IV}(H_2O)_2$
(1)$Fe^{III}(H_2O)$(*t*-$BuOO^{\cdot}$)	(1)$Fe^{IV}(H_2O)$(HO) or (+·1)$Fe^{IV}(H_2O)$(HO)
(1)$Fe^{III}(HO^-)$(*t*-$BuOO^{\cdot}$)	(1)Fe^{IV}(HO)2 or (+·1)Fe^{IV}(HO)2

ability of experimental points beyond pD 10 (see Results) and the large number of individual rate and equilibrium constants affected by a change in solvent from H_2O to D_2O. This underscores the futility of trying to interpret a "solvent isotope effect" determined from comparing k_{obsd} values at one pH(D) value with such complex systems, as has been attempted in the past.[20]

Mechanisms of Reactions. A study of the reaction of H_2O_2 with lyate species ligated $[(2)Fe^{III}]^+$, in aqueous solution, has recently appeared.[21] It was found at low pH that k_{ly} is pH-independent, $k_{ly}^H/k_{ly}^D = 3.0$, and that there was no catalysis by RCO_2^- or RCO_2H species. Like observations ($k_{ly}^H/k_{ly}^D = 2.7$) pertain to the reaction of *t*-BuOOH with (1)$Fe^{III}(H_2O)_2$ at low pH. Oxygen transfer from ROOH or RCO_3H to iron(III) porphyrins is generally considered to provide iron(IV)–oxo porphyrins and iron(IV)–oxo porphyrin π-cation radical species. The mechanism of the reaction of (2)$Fe^{III}(H_2O)_2$ with H_2O_2 at low pH was discussed with the assumption of the formation of the oxo species as products (pp 6069–6071 of ref 21).

The electrochemical studies of the previous paper in this issue[14] established the structures, acid dissociation constants, and potentials of Scheme IV. Examination of Scheme IV shows that the oxygen ligands of iron porphyrins in water are H_2O and HO^-. This is so regardless of the oxidation state. Questions arise as to what are the immediate products in the oxidation of iron(III) tetraphenylporphyrins by alkyl and acyl hydroperoxides. Is the thermodynamically most stable product (Scheme IV) the immediate product of the oxidation reaction? Does the oxo species play any role in these reactions?

A comparison of the inventories of the number of protons present in the *t*-BuOOH iron(III) porphyrin complexes, which yield a product at various pH, to the number of protons present in the thermodynamically most stable oxidation products shows (Scheme V) that the latter contain an additional proton. Therefore, in order to form the most stable product (regardless of the pH or whether the mechanism involves homolytic or heterolytic O–O bond scission) an additional proton must be included in the transition state. However, neither general nor specific acid catalysis is observed at any pH. Therefore, the initial product of these reactions must contain one less proton than does the thermodynamically most stable form of the product.

(20) Traylor, T. G.; Xu, F. *J. Am. Chem. Soc.* **1990**, *112*, 178.
(21) Panicucci, R.; Bruice, T. C. *J. Am. Chem. Soc.* **1990**, *112*, 6063.

Scheme VI

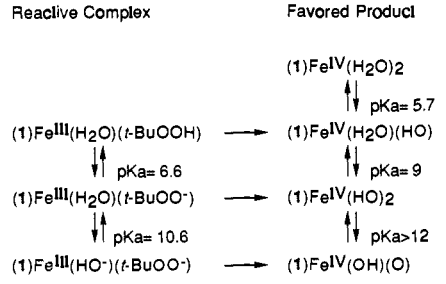

Since (1)$Fe^{IV}(H_2O)$(OH) is a base of a diaquo acid with $pK_a \sim 6.0$, it is not unduly unstable when created in the low pH-independent region which extends to pH 3. The products formed in the homolytic reaction are the thermodynamically favored species at the next highest pH region of the log k_{ly} vs pH profile (compare Schemes VI and IV). The formation of iron–oxo species is allowed only above pH $\sim$ 6 since ((1)$Fe^{IV}(OH)_2$ and (1)-$Fe^{IV}(O)(H_2O)$ possess the same proton inventory, though the former is expected to be more stable.

For any heterolytic reaction the instability of *t*-BuO^- (pK_a of *t*-BuOH is $\sim$ 17), particularly at low and intermediate pH values, must be considered. The reaction of eq 6 (low pH) would be highly disfavored when compared to that of eq 7 even though the species

$$(1)Fe^{III}(H_2O)(t\text{-BuOOH}) \rightarrow (1^{\cdot+})Fe^{IV}(H_2O)(OH) + t\text{-}BuO^- \quad (6)$$

$$(1)Fe^{III}(H_2O)(t\text{-BuOOH}) \rightarrow (1^{\cdot+})Fe^{IV}(H_2O)(O) + t\text{-BuOH} \quad (7)$$

$(1^{+\cdot})Fe^{IV}(H_2O)(O)$ is a base of an acid with $pK_a \geq 9.0$. To obviate the formation of $(1^{+\cdot})Fe^{IV}(H_2O)(O)$ one might expect general acid catalysis as shown in eq 8. However, the reaction is not catalyzed by H_3O^+ or general acids (AH).

$$(1)Fe^{III}(H_2O)(t\text{-BuOOH}) + AH \rightarrow (1^{\cdot+})Fe^{IV}(H_2O)(OH) + t\text{-BuOH} + A: \quad (8)$$

Though there is neither general nor specific acid–base catalysis at the low pH plateau, a deuterium solvent kinetic isotope effect of 2.7 is observed. For a heterolytic mechanism, such an isotope effect might be expected if proton transfer from $(1^{+\cdot})Fe^{IV}(H_2O)$(OH) to *t*-$BuO^-$ is rate controlling or if O–O bond heterolysis and proton transfer are concerted (eq 7). Reactions, which do not involve rate-determining proton transfer, commonly exhibit solvent kinetic isotope effects (k^H/k^D) of 1.2–1.4. The remaining deuterium solvent kinetic isotope [2.7/(1.2 or 1.4)] is equivalent to a change in free energy of activation ($\Delta\Delta G^*$) of 0.47–0.38 kcal M^{-1}. This is equivalent to a change in potential for $1e^-$ oxidation of the iron porphyrin of only 20–16 mV on transfer from H_2O to D_2O. The reaction of eq 9 consists of an e^- transfer and O–O bond homolysis. If e^- transfer precedes O–O bond breaking, then

$$(1)Fe^{III}(H_2O)(t\text{-BuOOH}) \rightarrow (1)Fe^{IV}(H_2O)(OH) + t\text{-}BuO^{\cdot} \quad (9)$$

the value of k_{ly}^H/k_{ly}^D can be explained by a very small change in the potential of the iron(III) moiety of (1)$Fe^{III}(H_2O)$(*t*-BuOOH). Electrochemical studies[14] indicate that potential changes on transfer from H_2O to D_2O must not be much greater than 10 mV such that the entire isotope effect cannot be explained by a potential change on transfer from H_2O to D_2O. It is worth noting that the larger pK_a^H/pK_a^D for iron(IV) species as compared to iron(III) species indicates that there must be some change in potential on transfer from H_2O to D_2O. It would appear that at low pH the deuterium solvent kinetic isotope effect can be explained either by the heterolytic mechanism of eq 7 or, alternatively, the homolytic mechanism of eq 10a,b (where homolysis

$$(1)Fe^{III}(H_2O)(t\text{-BuOOH}) \rightarrow \{(1)Fe^{IV}(H_2O)(OH) + t\text{-}BuO^{\cdot}\} \quad (10a)$$

$$\{(1)Fe^{IV}(H_2O)(OH) + t\text{-}BuO^{\cdot}\} \rightarrow (1^{\cdot+})Fe^{IV}(H_2O)(O) + t\text{-BuOH} \quad (10b)$$

Scheme VII

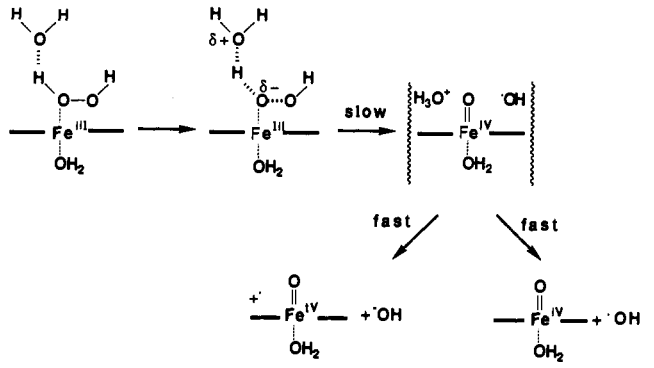

Scheme VIII

$$(1)Fe^{III}(H_2O)(t\text{-BuOO}) \longrightarrow (1)Fe^{IV}(O)(H_2O) + t\text{-BuO}\cdot$$
$$(1)Fe^{IV}(O)(H_2O) + H^+ \longrightarrow (1)Fe^{IV}(OH)(H_2O)$$
$$t\text{-BuO}\cdot \longrightarrow (CH_3)_2C{=}O + CH_3\cdot$$
$$(1)Fe^{IV}(OH)(H_2O) + CH_3\cdot \longrightarrow (1)Fe^{III}(H_2O)_2 + CH_3OH$$

Scheme IX

$$t\text{-BuO}\cdot + t\text{-BuOOH} \longrightarrow t\text{-BuOH} + t\text{-BuOO}\cdot$$
$$t\text{-BuOO}\cdot \longrightarrow t\text{-BuO}\cdot + 1/2\ O_2$$

Scheme X

$$(1)Fe^{III}(H_2O)_2 + t\text{-BuOOH} \longrightarrow (\cdot{+}1)Fe^{IV}(O)(H_2O) + t\text{-BuOH}$$
$$(\cdot{+}1)Fe^{IV}(O)(H_2O) + t\text{-BuOOH} \longrightarrow (1)Fe^{IV}(OH)(H_2O) + t\text{-BuOO}\cdot$$
$$t\text{-BuOO}\cdot \longrightarrow t\text{-BuO}\cdot + 1/2O_2$$
$$t\text{-BuO}\cdot \longrightarrow (CH_3)_2CO + CH_3\cdot$$
$$(1)Fe^{IV}(OH)(H_2O) + CH_3\cdot \longrightarrow (1)Fe^{III}(H_2O)_2 + CH_3OH$$

and H• transfer are both partially rate controlling). With either mechanism, contributions to k_{1y}^H/k_{1y}^D from secondary isotope effects and small potential changes are also likely. In a previous publication the homolytic mechanism of Scheme VII was suggested (for the (2)$Fe^{III}(H_2O)_2$-catalyzed decomposition of HOOH at low pH).[21] This mechanism may be questioned, in the light of the electrochemical results,[14] on the basis that the immediate product (2)$Fe^{IV}(=O)(H_2O)$ [taken in analogy with (1)$Fe^{IV}(=O)(H_2O)$] is expected to be thermodynamically unstable at low pH. A homolytic mechanism is preferred on the basis of the decided indifference to leaving group ability in the reaction of weakly acidic hydroperoxides with (porph)$Fe^{III}(X_2)$ species.[2,4]

Above the pH-independent region at low pH there is no evidence of a kinetic solvent deuterium isotope effect (loc. cit.). Here the hydroperoxy proton has become dissociated (IIH and II^- in Scheme II). The reactions are clearly homolytic as shown by product studies.[3,4,18] From pH 4–13 the reaction of *t*-BuOOH with (1)$Fe^{III}(X)_2$ or (2)$Fe^{III}(X)_2$ provides acetone in ~90% yield and methanol in 90% and >50% yields, respectively, based on [*t*-BuOOH] used.[3,4,18] The simplest homolytic sequence (Scheme VIII) provides acetone in a yield of 100%. The radicals *t*-BuOO• and

$$t\text{-BuO}^\bullet \rightarrow (CH_3)_2C{=}O + CH_3^\bullet$$

$$(1)Fe^{IV}(OH)(H_2O) + CH_3^\bullet \rightarrow (1)Fe^{III}(H_2O)_2 + CH_3OH$$

and *t*-BuO• have been spin trapped in the course of the reaction of *t*-BuOOH with (1)$Fe^{III}(X)_2$[4] (Scheme IX). Assuming that 90% *t*-BuOOH is consumed in Scheme VIII and 10% in Scheme IX there would be observed the experimental 90% yield of acetone. The simplest presentation of a heterolytic mechanism for O–O bond cleavage (Scheme X) provides 50% acetone. Inclusion of one cycle of the reactions of Scheme IX reduces the yield of $(CH_3)_2CO$ and MeOH to 25% (Scheme XI). Thus, a heterolytic mechanism is incompatible with our experimentally observed yields of >90% formation of $(CH_3)_2CO$ and MeOH. The mechanism involving homolytic O–O bond cleavage must be favored. Scheme I correctly predicts the observed material balance, at least in the pH range 3–12.

Scheme XI

$$(1)Fe^{III}(H_2O)_2 + t\text{-BuOOH} \longrightarrow (\cdot{+}1)Fe^{IV}(O)(H_2O) + t\text{-BuOH}$$
$$(\cdot{+}1)Fe^{IV}(O)(H_2O) + t\text{-BuOOH} \longrightarrow (1)Fe^{IV}(OH)(H_2O) + t\text{-BuOO}\cdot$$
$$t\text{-BuOO}\cdot \longrightarrow t\text{-BuO}\cdot + 1/2O_2$$
$$t\text{-BuO}\cdot + t\text{-BuOOH} \longrightarrow t\text{-BuOH} + t\text{-BuOO}\cdot$$
$$t\text{-BuOO}\cdot \longrightarrow t\text{-BuO}\cdot + 1/2O_2$$
$$t\text{-BuO}\cdot \longrightarrow (CH_3)_2CO + CH_3\cdot$$
$$(1)Fe^{IV}(OH)(H_2O) + CH_3\cdot \longrightarrow (1)Fe^{III}(H_2O)_2 + CH_3OH$$

Scheme XII

$$Fe^{3+} + HO_2^\cdot \rightleftharpoons Fe^{3+}HO_2^- \quad (i)$$
$$Fe^{3+}HO_2^- \longrightarrow FeO^{3+} + HO^- \quad (ii)$$
$$FeO^{3+} + HO_2^- \longrightarrow Fe^{3+} + O_2 + HO^- \quad (iii)$$

Scheme XIII

$$H_2O_2 + Fe^{3+} \longrightarrow Fe^{2+} + H^+ + HO_2^\bullet \quad \text{(Initiation)}$$
$$Fe^{2+} + H_2O_2 \longrightarrow Fe^{3+} + HO^- + HO^\bullet \quad \text{(Propagation)}$$
$$HO^\bullet + H_2O_2 \longrightarrow H_2O + HO_2^\bullet \quad \text{(Propagation)}$$
$$HO_2^\bullet + Fe^{3+} \longrightarrow Fe^{2+} + H^+ + O_2 \quad \text{(Propagation)}$$
$$HO_2^\bullet + Fe^{2+} \longrightarrow Fe^{3+} + HO_2^- \quad \text{(Termination)}$$

The reaction of ferric iron with *tert*-butyl hydroperoxide at pH(D) 1–4, in the presence of ABTS, is first-order in both [*t*-BuOOH(D)] and [Fe^{III}] and provides the stoichiometrically required yields of two $ABTS^{\bullet+}$ species per each *t*-BuOOH(D) consumed (30 °C, μ = 0.2). Under these conditions one cannot have Fenton chemistry. The second-order rate constant (k_{1y}) is pH-independent in the pH(D) range investigated and k_{1y}^H/k_{1y}^D = 2.0.

No prior mechanistic studies have been reported in the literature of Fe^{III}-catalyzed reduction of *tert*-butyl peroxide in aqueous solvents. Studies of the Fe^{III}–H_2O_2 system are abundant, and divergent views exist on the mechanisms of these reactions. A detailed study of the decomposition of H_2O_2 by Fe^{III}(edta) [edta = ethylenediamine tetraacetate] has been carried out by Oakes et al.[22] Their structural and kinetic studies indicate a two-step mechanism where preequilibrium complexation of the peroxide is followed by rate-determining breakdown of the complex. Hydroxyl radicals were observed in the reaction mixtures by spin trapping, and no buildup of high-valent Fe–oxo species was detected. Thus, the results are consistent with homolytic O–O bond cleavage in the rate-determining step. Catalytic decomposition of H_2O_2 by ferric ions, in the absence of EDTA, at low pH (pH 2.1, 27 °C, μ = 0.25), has also been reported.[23,24] Kremer[23] finds that kinetic analysis of his data supports a "complex" mechanism (Scheme XII) involving steady-state formation of two intermediates. The first was assigned to an iron(III)–hydroperoxy complex (Fe^{3+}–HO_2^- of Scheme XII) and the second to a high-valent Fe–oxo species (FeO^{3+}). Hydroxyl radicals were not considered to be intermediates. Hydroxyl radicals can be detected, and Walling[24] favors a mechanism in which HO• are intermediate in a free-radical chain mechanism (Scheme XIII).

The discrepancy concerning the validity of Scheme XII vs Scheme XIII appears to result from the interpretation of peroxy complex formation as being synonymous with an ionic mechanism (where heterolytic cleavage of the O–O bond of the complexed peroxide occurs) and the detection of the presence of hydroxyl radicals in the reaction mixtures as supporting a radical chain mechanism. The mechanism represented by steps a, b, c, and d of Scheme XIV reconciles both these apparently conflicting sets of observations.

(22) Francis, K. C.; Cummins, D.; Oakes, J. *J. Chem. Soc., Dalton Trans.* **1985**, 493.
(23) Kremer, M. L. *Int. J. Chem. Kinet.* **1985**, *17*, 1299 and references therein.
(24) Walling, C. *Acc. Chem. Res.* **1975**, *8*, 125 and references therein.

Scheme XIV

$$Fe^{III} + H_2O_2 \rightleftharpoons Fe^{III}H_2O_2 \quad (a)$$
$$Fe^{III}H_2O_2 \longrightarrow Fe^{IV}OH + HO^{\bullet} \quad (b)$$
$$HO^{\bullet} + H_2O_2 \longrightarrow H_2O + HO_2^{\bullet} \quad (c)$$
$$Fe^{IV}OH + HO_2^{\bullet} \longrightarrow Fe^{III} + H_2O + O_2 \quad (d)$$
$$HO^{\bullet} + ABTS + H^+ \longrightarrow H_2O + ABTS^{\bullet+} \quad (e)$$
$$Fe^{IV}OH + ABTS + H^+ \longrightarrow Fe^{III} + H_2O + ABTS^{\bullet+} \quad (f)$$

In our system, $Fe^{IV}OH$ and $HO^{\bullet}$, formed as primary products, would be trapped by ABTS so that steps (c) and (d) of Scheme XIV would be replaced by (e) and (f). At low pH k_{ly}^H is independent of pH, and (k_{ly}^H/k_{ly}^D) is much the same for Fe^{III} (1.9) and (1)$Fe^{III}(X)_2$ (2.7) and is comparable to $k_{ly}^H/k_{ly}^D = 3.0$ for the reaction of H_2O_2 with (2)$Fe^{III}(X)_2$. A common mechanism for these reactions is suggested.

In the reactions with *t*-BuOOH the value of k_{ly}^H with Fe^{III} is 5-fold greater than is k_{ly}^H for the reaction with (1)$Fe^{III}(X)_2$ at low pH. Thus at low pH, porphyrin ligation actually appears to impede the reaction of Fe^{III} with *t*-BuOOH. This may be partially due to the availability of three times as many sites for coordination of hydroperoxide on Fe^{III} as compared to (1)$Fe^{III}(X)_2$. In any case, (1)$Fe^{III}(X)_2$ does not react with *t*-BuOOH through a pathway any more favorable than that for the reaction of Fe^{III} with *t*-BuOOH (Scheme XIII, steps (a), (b), (e), and (f)). Therefore, at low pH homolytic cleavage of the O–O bond of *t*-BuOOH ligated to (1)$Fe^{III}(X)_2$ appears to be the most favorable pathway available for its decomposition.

Acknowledgment. We express our gratitude to the National Institutes of Health for support of this study.

Investigation of Intramolecular Interactions in *n*-Alkanes. Cooperative Energy Increments Associated with GG and GTG′ Sequences

Seiji Tsuzuki,[1a] Lothar Schäfer,*[,1b] Hitoshi Gotō,[1c] Eluvathingal D. Jemmis,[1d] Haruo Hosoya,[1e] Khamis Siam,[1b,f] Kazutoshi Tanabe,[1a] and Eiji Ōsawa*[,1c]

Contribution from the National Chemical Laboratory for Industry, Tsukuba, Ibaraki 305, Japan, Department of Chemistry, University of Arkansas, Fayetteville, Arkansas 72701, Department of Knowledge-Based Information Engineering, Toyohashi University of Technology, Toyohashi 441, Japan, School of Chemistry, University of Hyderabad, Central University P. O., Hyderabad 500134, India, and Department of Chemistry, Faculty of Science, Ochanomizu University, Bunkyo-ku, Tokyo 112, Japan. *Received July 16, 1990*

Abstract: Energies of rotational isomers of *n*-alkanes are largely determined by the number of individual gauche bonds (G). However, according to molecular mechanics calculations (MM2), within a group of rotamers with equal number of G bonds, there are characteristic energy variations due to cooperative effects involving sequences of several bonds. For example, the energy is increased by inserting a trans bond (T) between two consecutive G bonds of the same sign (e.g., TGGG < GTGG in *n*-heptane), and special long-range repulsive interactions seem to exist between G and G′, a gauche bond of opposite sign, in a GTG′ sequence (e.g., GTG < GTG′ in *n*-hexane). With use of ab initio MP4SDQ/6-31G*//6-31G* energies and geometries of ethane to *n*-hexane, including all rotamers, a 0.16 kcal/mol stabilizing energy increment is found to be characteristic for GG sequences. The potential source of this increment is found in nonbonded *attractive* interactions between 1,5-CH_3/CH_3, -CH_3/CH_2, and -CH_2/CH_2 groups, which are specific for GG but not for other combinations, such as GT, TT, or GG′. In addition, a 0.12 kcal/mol destabilizing energy increment is found to be associated with GTG′ sequences relative to GTG. It is rationalized by unfavorable nonbonded interactions that can be relaxed in GTG but not in GTG′ due to symmetry constraints. Whereas these cooperative energy increments are small for a single GG or GTG′ sequence, their accumulation in polymers can be considerable. The GG′ equilibrium structure of *n*-pentane belongs to the C_1 point group due to unequal C–C–C–C dihedral angles (±63 and ∓95°). A symmetric GG′ conformer (C_s) is 0.28 kcal/mol above the GG′ energy minimum and is identified as a saddle point. In contrast to a generally accepted rule, the lack of local symmetry in GG′ sequences implies the possible existence of more than 3^n rotamers for alkanes with *n* rotatable bonds. Good agreement is found for the order of MM2 and ab initio conformational energies. The results of this study are also of general interest, because they demonstrate one of the factors that can contribute to errors in conformational energies at the SCF level: Different conformations of a molecule may differ in stabilizing van der Waals interactions whose neglect leads to errors in all energy calculations that do not include dispersion forces.

The success of molecular modeling based on empirical potential energy calculations[2] depends on the ability of the computational techniques to correctly reproduce intra- and intermolecular relative energies. The problem here is the sparsity of accurate conformational energies, experimental or theoretical, by which parameters of empirical potential functions can be determined.[3]

Among small *n*-alkanes, for example, only a few rotamer energies for *n*-butane and *n*-pentane in the vapor phase have been recorded in the literature (Table I). A glance at this table reveals that, in addition to the considerable scatter in the experimental gauche butane energies, there is a serious problem in that the experimental gauche energy decreases significantly in going from *n*-butane (about 870 cal/mol) to *n*-pentane (about 500 cal/mol), whereas ab initio calculations at certain higher levels consistently reproduce about 700 cal/mol for these molecules.[4] Current molecular mechanics force fields neglect these difficulties[5] and

(1) (a) NCLI. (b) University of Arkansas. (c) Toyohasi University of Technology (correspondence address). (d) University of Hyderabad. (e) Ochanomizu University. (f) Present address: Chemistry Department, Pittsburgh State University, Pittsburgh, KS 66762.

(2) Müller, K. *Chimia* **1984**, *38*, 249. Kollman, P. *Annu. Rev. Phys. Chem.* **1987**, *38*, 303. Cohen, N. C.; Blaney, J. M.; Humblet, C.; Gund, P.; Barry, D. C. *J. Med. Chem.* **1990**, *33*, 883.

(3) Burkert, U.; Allinger, N. L. *Molecular Mechanics*; American Chemical Society: Washington, D.C., 1982.

0002-7863/91/1513-4665$02.50/0